

ANNOTATION-EFFICIENT ACTIVE TEST-TIME ADAPTATION WITH CONFORMAL PREDICTION

Tingyu Shi¹

Fan Lyu²

Shaoliang Peng^{3*}

¹ Computer Science and Engineering, University of California San Diego

² New Laboratory of Pattern Recognition, Institute of Automation, Chinese Academy of Sciences

³ College of Computer Science and Electronic Engineering, Hunan University

ABSTRACT

Active Test-Time Adaptation (ATTA) improves model robustness under domain shift by selectively querying human annotations at deployment, but existing methods use heuristic uncertainty measures and suffer from low data selection efficiency, wasting human annotation budget. We propose Conformal Prediction Active TTA (CPATTA), which first brings principled, coverage-guaranteed uncertainty into ATTA. CPATTA employs smoothed conformal scores with a top- K certainty measure, an online weight-update algorithm driven by pseudo coverage, a domain-shift detector that adapts human supervision, and a staged update scheme balances human-labeled and model-labeled data. Extensive experiments demonstrate that CPATTA consistently outperforms the state-of-the-art ATTA methods by around 5% in accuracy. Our code and datasets are available at <https://github.com/tingyushi/CPATTA>.

Index Terms— Domain Shift, Test-Time Adaptation, Active Test-Time Adaptation, Conformal Prediction

1. INTRODUCTION

Test-Time Adaptation (TTA) aims to update pretrained models on-the-fly using unlabeled test-time data, enabling them to handle domain shifts where the distribution of test samples differs from the training set. Such domain shifts are common in real-world applications, including autonomous driving under varying weather conditions [1, 2], cross-hospital MRI imaging with different devices [3, 4], and speech recognition with diverse accents and noise [5, 6]. Despite its growing popularity [7–10], TTA often suffers from suboptimal real-time and post-adaptation performance due to the lack of ground-truth supervision. Inspired by Active Learning, the Active Test-Time Adaptation (ATTA) paradigm [11] introduces selective human annotations during adaptation, enabling models to leverage supervised signals for improved robustness.

Existing methods on ATTA propose diverse criteria for selecting human-annotated samples. SimATTA [11] employs fixed entropy upper and lower thresholds combined with incremental clustering to determine samples for human annotation. CEMA [12] uses a fixed entropy lower bound and a dynamically adjusted upper bound to select samples for human annotation. EATTA [13] looks for samples located at the border of the source and the shifted domain by perturbing the softmax scores. However, existing ATTA methods suffer from **low data selection efficiency**, as illustrated in Fig. 1. A substantial portion of the annotated samples turns out to be redundant, since they could already be correctly predicted by the model, leading to a significant waste of limited human supervision. Such inef-

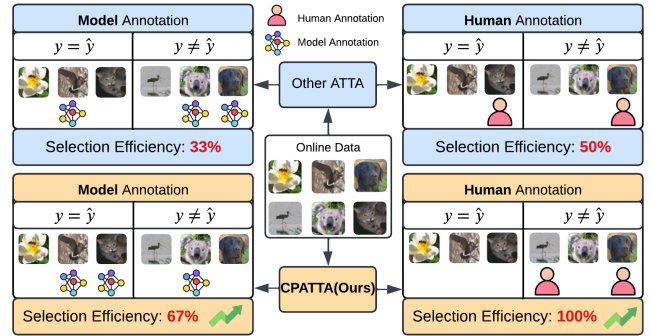


Fig. 1. Comparison between existing ATTA methods and CPATTA. Selection efficiency is defined as the fraction of useful samples: correct predictions for model-annotated data and incorrect predictions for human-annotated data. CPATTA achieves higher selection efficiency in both cases, enabling better real-time and post-adaptation performance under the same annotation budget.

ficiency not only diminishes the value of annotations but also constrains the overall adaptation performance. These limitations highlight the need for a more effective selection mechanism that can maximize the utility of human annotations during test-time adaptation.

To address the inefficiency of existing ATTA methods, a natural idea is to introduce a principled measure of uncertainty. **Conformal prediction (CP)** provides such a tool by transforming a model’s single-point output into a prediction set with statistical coverage guarantees. The size of this set reflects the model’s uncertainty, making CP an appealing candidate for guiding sample selection. *However, applying CP to ATTA is non-trivial.* Classical CP relies on the assumption that calibration and test data are exchangeable [14–16], which does not hold in ATTA since calibration data come from the source domain while test samples belong to a shifted domain. Although recent extensions of CP have relaxed this assumption, they still cannot provide valid guarantees under the dynamic and evolving conditions of test-time adaptation [17–19]. *This gap motivates us to explore how CP can be adapted and extended to improve annotation efficiency in the ATTA setting.*

In this paper, we propose **Conformal Prediction Active TTA** (CPATTA), a framework that integrates CP into ATTA. The core idea is to replace heuristic uncertainty measures with principled, coverage-guaranteed ones, and to adapt them to dynamic test-time environments. Specifically, CPATTA introduces three key components. First, it employs smoothed conformal scores and a top- K certainty measure to provide fine-grained uncertainty signals, enabling more efficient allocation of scarce human annotations and reliable pseudo-labeling. Second, it develops an online weight-update

*Corresponding author. Email: slpeng@hnu.edu.cn

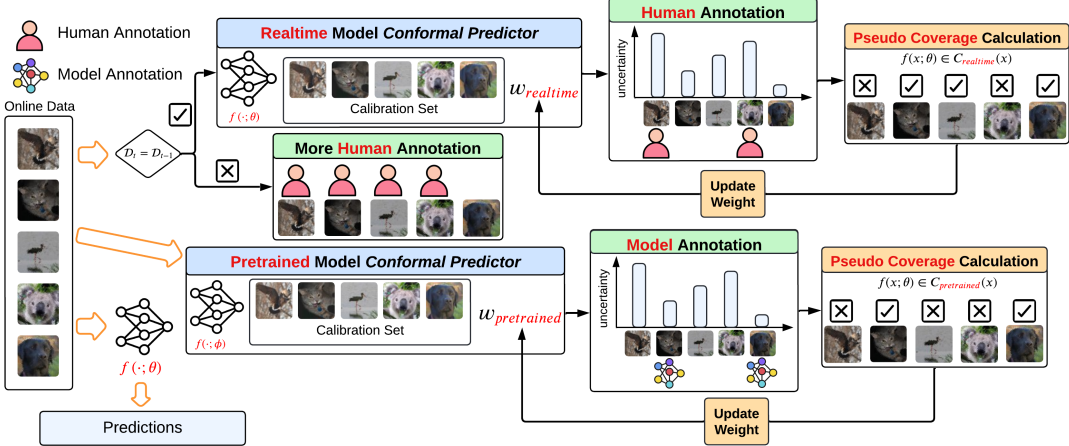


Fig. 2. Overview of CPATTA method. The real-time model $f(\cdot; \theta)$ makes the predictions right away when an online batch of data arrives. If CPATTA detects that current batch’s domain is different from the previous batch’s domain ($\mathcal{D}_t \neq \mathcal{D}_{t-1}$), the algorithm selects more data for human annotation to ensure the real-time performance. Two CPs provide uncertainty measures for each sample within the batch; human annotates uncertain samples while the model annotates certain samples. Then, CPATTA updates the weights of two CPs based on the pseudo coverages calculated from model predictions and prediction sets.

algorithm that leverages pseudo coverage as feedback to dynamically correct coverage under domain shifts, ensuring that uncertainty estimates remain calibrated to the user-chosen risk level. Third, CPATTA incorporates a domain-shift detector that increases human supervision when a new domain is encountered, preventing error accumulation at the onset of sudden distributional changes. Together, these designs yield an annotation strategy that is both efficient and reliable, leading to improved real-time and long-term adaptation performance. Experimental results show that our method outperforms existing ATTA methods.

2. METHOD

2.1. Problem Statement and Conformal Prediction

Let $f(\cdot; \phi)$ denote a model pretrained on a source domain dataset \mathcal{D}_S . At deployment, a real-time model $f(\cdot; \theta^t)$ is initialized with the pretrained parameters, i.e., $\theta^0 = \phi$. During test-time, unlabeled data arrive sequentially in mini-batches $\mathcal{B}^t = \{x_1^{S'}, \dots, x_{N_t}^{S'}\}$, drawn from a shifted target domain S' . The key challenge of ATTA is to adapt $f(\cdot; \theta^t)$ to this evolving target domain under a limited annotation budget. Specifically, at each step t , the model receives an unlabeled batch \mathcal{B}^t , selects a subset of samples for human annotation while another subset are pseudo-labeled by the model itself, and then updates its parameters from θ^t to θ^{t+1} using both human- and model-annotated data. The objective of ATTA is to maximize predictive performance by efficiently utilizing limited human supervision and continuously improving the deployed model in real time.

Existing ATTA methods suffer from low data selection efficiency, which makes the choice of samples for annotation a critical issue. Conformal Prediction (CP) offers a classical framework to quantify model uncertainty and guide sample selection. CP augments a predictor with prediction sets by leveraging a small-size labeled calibration set $\mathcal{D}_{cal} = \{(x_i, y_i)\}_{i=1}^n$ and a nonconformity score function \mathcal{S} . For a test input x_{n+1} , the prediction set is

$$\mathcal{C}(x_{n+1}) = \{y \in \mathcal{Y} | \mathcal{S}(x_{n+1}, y) \leq \tau\}, \quad (1)$$

where τ is the quantile conformal threshold.

$$\tau = \text{Quantile}_{1-\alpha}(\{\mathcal{S}(x_i, y_i)\}_{i=1}^n). \quad (2)$$

For a classification problem, a typical choice of \mathcal{S} is one minus the softmax score of the correct label. Under the exchangeability (same

distribution) assumption between calibration and test data, CP guarantees coverage with high probability [14]: $1 - \alpha \leq \mathbb{P}(y \in \mathcal{C}(x)) \leq 1 - \alpha + \frac{1}{1+n}$, where n is the calibration set size. $\mathcal{C}(x)$ serves as a measure of uncertainty, where larger sets indicate lower uncertainty. Although CP leverages a small subset of source-domain data, these samples are not reused for training but only for calibrating conformal predictors to estimate prediction uncertainty. *In test-time applications where annotation resources are critical, such as autonomous driving with safety risks, or medical imaging with costly expert labeling, this calibration reduces redundant human annotations and improves real-time as well as post-adaptation performance.*

However, this guarantee relies on exchangeability assumption, which is violated in ATTA because calibration data are drawn from the source domain while test batches come from a shifted domain. This mismatch creates a **coverage gap** between the target and actual coverage. Although weighted extensions of CP [17, 18] attempt to recover coverage guarantees by reweighting samples, they depend on accurate weight estimation, which is infeasible under the dynamic nature of ATTA. Therefore, existing CP methods cannot be directly applied to ATTA, and *this limitation motivates us to design a new weight-estimation algorithm that ensures valid coverage and reliable sample selection in ATTA*.

2.2. Uncertainty-Guided Annotation with CP

Standard CP relies on prediction set size as an uncertainty proxy, which is too coarse for ATTA. We instead adopt smoothed prediction sets [20], converting hard set membership into soft inclusion scores and yielding more fine-grained uncertainty signals that adapt to dynamic test-time shifts. Given a normalized nonconformity score function \mathcal{S} , the soft score of including label y for input x is

$$E(x, y; \tau) = \sigma((\tau - \mathcal{S}(x, y)) / T), \quad (3)$$

where $\sigma(x) = \frac{1}{1+e^{-x}}$. T represents temperature. For a test input x with label space $\mathcal{Y} = \{1, \dots, L\}$, we sort labels in descending order

$$E(x, y_{(1)}; \tau) \geq E(x, y_{(2)}; \tau) \geq \dots \geq E(x, y_{(L)}; \tau), \quad (4)$$

and define the top- K certainty score as

$$\text{Cert}_K(x; \tau) = \mathbb{E}_{k \in [1, K]} E(x, y_{(k)}; \tau), \quad (5)$$

which reflects how strongly the model supports its most plausible labels, which is more informative compared to the hard CP.

Second, we leverage two complementary conformal predictors: one based on the pretrained model $f(\cdot; \phi)$ and one on the real-time adapted model $f(\cdot; \theta^t)$. For each test batch \mathcal{B}^t , these predictors yield thresholds τ_{pre} and τ_{rt} , from which we compute

$$\text{Cert}_K^{\text{pre}}(x) = \text{Cert}_K(x; \tau_{\text{pre}}), \quad \text{Cert}_K^{\text{rt}}(x) = \text{Cert}_K(x; \tau_{\text{rt}}). \quad (6)$$

Annotation is then allocated by sending the N_{human} least-certain samples under the real-time predictor to human annotators, while the N_{model} most-certain ones under the pretrained predictor receive pseudo-labels. The selected samples are stored in human buffer Buf_H and model buffer Buf_M for subsequent parameter updates.

Finally, to adapt annotation effort to domain dynamics, we integrate a domain-change detector. Specifically, we employ the Domain Shift Signal (DSS) [21] to test whether the current batch \mathcal{B}^t originates from a new domain. If a shift is detected, we temporarily increase the human annotation budget from N_{human} to $N'_{\text{human}} \geq N_{\text{human}}$, reflecting the reduced reliability of prior knowledge and accelerating adaptation at the onset of new domains.

2.3. Adaptive Weighting for CP in ATTA

Although uncertainty-guided annotation improves efficiency, valid coverage is still required for reliable adaptation. Since calibration data come from the source domain, the exchangeability assumption of classical CP is violated under domain shift (Sec. 2.1). To address this, we introduce a dynamic weighting mechanism that updates CP online during adaptation.

Pseudo Coverage as Feedback. Since ground-truth labels are unavailable at test time, true coverage cannot be computed. We thus define *pseudo coverage*, which treats the real-time model’s prediction as a surrogate label. For batch \mathcal{B}^t , the pseudo coverage of real-time and pretrained CPs is

$$PC_{\text{rt}}^t = \mathbb{E}_{x \in \mathcal{B}^t} \mathbb{1}[h(f(x; \theta^t)) \in C_{\text{rt}}^t(x)], \quad (7)$$

$$PC_{\text{pre}}^t = \mathbb{E}_{x \in \mathcal{B}^t} \mathbb{1}[h(f(x; \theta^t)) \in C_{\text{pre}}^t(x)], \quad (8)$$

where $h(f(x; \theta^t))$ is the predicted label. These values act as online feedback, revealing whether each CP under- or over-covers relative to the target level.

Online Weight Updates. Guided by pseudo coverage, we update the weights w_{rt}^t and w_{pre}^t assigned to real-time and pretrained CPs. Instead of fixed weights, we employ an exponential update rule that decreases weights when under-coverage is detected and increases them when over-coverage occurs, thereby steering coverage towards $1 - \alpha$. For the real-time CP, the update is

$$w_{\text{rt}}^t = \frac{w_{\text{rt}}^{t-1}}{T_{\text{rt}}^t}, \quad T_{\text{rt}}^t = \exp[(1 - \alpha) - PS_{\text{rt}}^{t-1}] \cdot T_{\text{rt}}^{t-1}, \quad (9)$$

with a symmetric update for w_{pre}^t . This enables CP to self-calibrate under evolving domains using only unlabeled feedback.

Coverage Guarantee. Following the theoretical framework of weighted CP [17, 18], our adaptive weighting scheme satisfies the coverage bound:

$$\begin{aligned} 1 - \alpha - \frac{w}{nw + 1} \sum_{i=1}^n d_{\text{TV}}(Z, Z^i) &\leq \mathbb{P}(x \in \mathcal{C}(x)) \quad (10) \\ &\leq 1 - \alpha + \frac{1}{nw + 1} + \frac{w}{nw + 1} \sum_{i=1}^n d_{\text{TV}}(Z, Z^i), \end{aligned}$$

where d_{TV} is total variation distance, $Z = ((x_i, y_i))_{i=1}^{n+1}$, Z^i swaps (x_i, y_i) with (x_{n+1}, y_{n+1}) , and we can substitute w with w_{rt}^t or w_{pre}^t . In essence, pseudo coverage serves as an online correction signal, keeping CP coverage near the target level despite domain shift.

2.4. Model Update

After each test batch is processed, the real-time model parameters are updated before the next batch arrives. The training objective combines cross-entropy losses from both buffers:

$$\mathcal{L}_H(\theta) = \mathbb{E}_{(x, y) \in \text{Buf}_H} - \log(\text{softmax}(f(x; \theta))_y), \quad (11)$$

$$\mathcal{L}_M(\theta) = \mathbb{E}_{(x, \hat{y}) \in \text{Buf}_M} - \log(\text{softmax}(f(x; \theta))_{\hat{y}}). \quad (12)$$

$\text{softmax}(\cdot)_y$ denotes the softmax probability assigned to label y .

To balance reliability and efficiency, we adopt a two-stage update with buffer-specific learning rates. First, parameters are updated using human-labeled data with rate η_H

$$\theta^{t+\frac{1}{2}} = \theta^t - \eta_H \nabla_{\theta} \mathcal{L}_H(\theta^t), \quad (13)$$

and then further updated with model-labeled data using rate η_M :

$$\theta^{t+1} = \theta^{t+\frac{1}{2}} - \eta_M \nabla_{\theta} \mathcal{L}_M(\theta^{\frac{1}{2}}). \quad (14)$$

This staged update scheme reflects the design principle of trust but expand. Reliable human supervision anchors the model update, while additional pseudo-labeled data broaden adaptation at low cost. The method ensures that human annotations dominate parameter correction, whereas model labels serve as auxiliary signals that accelerate adaptation without overwhelming reliability.

2.5. Discussion: CPATTA vs. Existing Nonexchangeable CP

Prior extensions of CP under distribution shift typically rely on fixed or heuristic weighting. For instance, weighted CP [17, 18] rebalances calibration scores via predefined constants or geometric decay. Such static schemes cannot adapt to evolving domains in ATTA, where calibration-target distribution similarity changes across batches. Similarly, QTC [19] adjusts thresholds using unlabeled test data, but depends on stable model predictions. In ATTA, the model is continuously updated and errors accumulate, making these scores unreliable and the resulting coverage unstable.

In contrast, CPATTA leverages pseudo coverage as an online feedback signal and adaptively reweights CP to track distribution drift. This design enables principled and dynamic coverage control, forming a key distinction from existing nonexchangeable CP approaches and completing our method.

3. EXPERIMENTS

Experiment Details. We evaluate on three domain shift datasets, including PACS, VLCS and Tiny-ImageNet-C. PACS [22] consists of 4 domains (Photo, Art painting, Cartoon, Sketch) spanning 7 categories. VLCS [23] combines 4 other datasets with 5 classes, providing natural distribution shifts across domains. Tiny-ImageNet-C [24] extends Tiny-ImageNet with 200 classes by adding 15 corruption types at 5 severity levels, and we use severity 5 for the experiment. Evaluation is based on real-time accuracy, post-adaptation accuracy, and coverage gap. For PACS and VLCS, we sample 50 images per class from the source domain, forming calibration sets of 350 and 250 images, respectively. For Tiny-ImageNet-C, we select 3 images per class, yielding 600 images. For PACS and VLCS, we select the 3 most uncertain samples per batch for human annotation, while for Tiny-ImageNet-C we select 2. Accordingly, the human annotation budget is capped at 300 for PACS/VLCS and 3000 for Tiny-ImageNet-C across all methods to ensure fair comparison. We set $K = 1$ for top- K certainty score for all 3 datasets. The backbone model is ResNet-18 [25], which is pretrained on domain P , C , and $brightness$ for the three datasets, respectively.

Table 1. Real-Time and Post-Adaptation Accuracy on PACS, VLCS and Tiny-ImageNet-C. **Acc** refers to the overall accuracy.

Method	PACS					VLCS					Tiny-ImageNet-C	
	Real-Time		Post-Adapt			Real-Time		Post-Adapt			Real-Time	Post-Adapt
	A	C	S	Acc	Acc	L	S	V	Acc	Acc	Acc	Acc
Tent [7]	67.19	68.98	67.09	67.64	75.06	46.26	41.22	55.72	47.91	56.90	12.69	13.86
CoTTA [9]	65.68	65.87	64.55	65.17	70.84	45.84	39.49	54.92	46.89	47.33	3.44	9.10
SimATTA [11]	72.56	49.36	72.49	65.99	77.85	65.38	59.78	63.71	62.80	71.97	33.30	41.81
CEMA [12]	51.56	66.98	67.01	63.20	76.45	55.18	43.39	49.35	48.91	63.93	32.09	41.58
EATTA [13]	70.07	69.16	65.60	67.89	75.07	44.56	39.48	53.14	45.88	54.22	13.65	15.57
CPATTA(Ours, $\alpha = 0.1$)	71.39	68.05	76.18	72.71	85.25	57.99	64.87	70.50	64.95	76.79	34.61	43.74
CPATTA(Ours, $\alpha = 0.2$)	73.10	70.01	79.51	75.26	87.13	58.11	61.88	73.34	64.96	77.72	34.61	43.73
CPATTA(Ours, $\alpha = 0.3$)	72.51	73.76	74.60	73.85	85.69	57.77	62.52	72.66	64.84	76.35	34.77	44.59

Table 2. Data selection efficiencies comparisons.

Method	PACS		VLCS		Tiny-ImageNet-C	
	Eff _H	Eff _M	Eff _H	Eff _M	Eff _H	Eff _M
SimATTA	47.60	67.60	57.04	64.78	79.25	50.00
CEMA	24.91	N/A	44.38	N/A	75.82	N/A
EATTA	53.71	90.71	58.38	63.60	62.90	32.31
CPATTA(Ours, $\alpha = 0.1$)	66.30	93.41	62.89	81.91	90.62	47.55
CPATTA(Ours, $\alpha = 0.2$)	65.94	93.65	61.86	85.11	90.62	47.55
CPATTA(Ours, $\alpha = 0.3$)	67.39	94.59	64.29	84.04	90.45	48.14

Compared Methods. We compare against two TTA methods, Tent [7] and CoTTA [9], and three ATTA methods, CEMA [12], SimATTA [11], and EATTA [13]. For Tent and CoTTA, we adopt the enhanced TTA protocol from [11], which grants access to additional randomly sampled labels. For CEMA, we retain only its selective mechanism, replacing foundation-model annotations with human annotations, so there are no model annotations for CEMA.

Real-Time and Post-Adaptation Accuracy. Table 1 reports real-time and post-adaptation accuracies on PACS, VLCS, and Tiny-ImageNet-C with different miscoverage levels ($\alpha = 0.1, 0.2, 0.3$). CPATTA achieves clear and consistent improvements across all benchmarks. On PACS, CPATTA with $\alpha = 0.2$ reaches 75.26% real-time accuracy and 87.13% post-adaptation accuracy, improving over SimATTA by nearly 9% in real-time and post-adaptation. On VLCS, CPATTA also delivers strong gains, with 64.96% real-time and 77.72% post-adaptation accuracy, outperforming CEMA and EATTA by over 15% and 20% respectively. Even on the challenging Tiny-ImageNet-C benchmark, CPATTA surpasses all ATTA baselines, achieving the best post-adaptation accuracy of 44.59%. These results demonstrate that CPATTA is not only more effective than SOTA methods but also more adaptable to diverse domain shifts.

Data Selection Efficiency. We formally define efficiency of human annotation(Eff_H) and model annotation(Eff_M) as follows:

$$\text{Eff}_H = \mathbb{E}_{(x,y) \in \text{Bf}_H} \mathbb{1}[y \neq \hat{y}], \quad (\text{Model Predicts Wrong}) \quad (15)$$

$$\text{Eff}_M = \mathbb{E}_{(x,y) \in \text{Bf}_M} \mathbb{1}[y = \hat{y}]. \quad (\text{Model Predicts Right}) \quad (16)$$

As shown in Table 2, CPATTA achieves the highest Eff_H across all datasets, while maintaining competitive or superior Eff_M. The results are stable across different α values, demonstrating CPATTA’s effectiveness in improving annotation efficiency in ATTA.

Coverage Gap. To evaluate the effectiveness of our adaptive weighting algorithm, we compare our CP with ExCP [15] and QTC [14] on VLCS. Fig. 3 reports the average coverage gap for both real-time model CP and pretrained model CP, along with real-time and post-adaptation accuracy. Across all α values, our CP consistently achieves the lowest coverage gap for both CPs. Furthermore, by ensuring better calibration, our method also delivers higher real-time and post-adaptation accuracy.

Ablation Study. We conduct ablation studies on PACS and VLCS, as shown in Table 3. RS denotes random selection. GD corresponds to geometric decay weights($w_i = \rho^{n+1-i}$, $\rho = 0.9$), following [17, 18]. AW denotes adaptive weighting (Sec. 2.3). The results

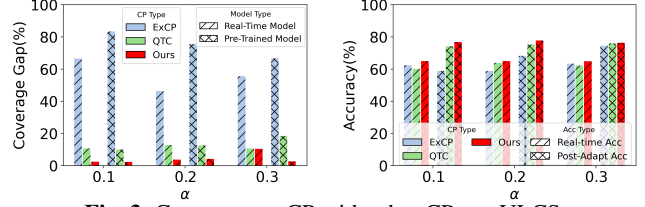


Fig. 3. Compare our CP with other CPs on VLCS

Table 3. Ablation Study on PACS and VLCS

	PACS		VLCS	
	Real-Time	Post-Adapt	Real-Time	Post-Adapt
RS	68.16	78.37	55.58	70.77
CP + GD	74.31	83.37	63.29	75.14
CP + AW	75.26	87.13	64.96	77.72

show that selection with CP improves performance over random selection, and incorporating adaptive weighting yields further gains, demonstrating the robustness of our approach.

Replay Experiment. To further show the effectiveness of CP in ATTA, we allow the compared methods access to the labeled calibration set as replay data during adaptation. Table 4 reports results on PACS. While SimATTA with replay improves accuracy on domain *A*, CPATTA achieves superior performance on the other two domains and obtains the best overall real-time and post-adaptation accuracy. This confirms that leveraging the calibration set through CP is more effective than using it as replay data.

Table 4. Replay Experiment on PACS

Method	Real-Time				Post-Adapt
	A	C	S	Acc	
SimATTA with Replay	74.32	50.64	72.77	66.92	79.14
CEMA with Replay	65.58	68.64	58.28	63.00	75.38
EATTA with Replay	69.97	69.07	65.59	67.65	74.85
CPATTA(Ours, $\alpha = 0.1$)	71.39	68.05	76.18	72.71	85.25
CPATTA(Ours, $\alpha = 0.2$)	73.10	70.01	79.51	75.26	87.13
CPATTA(Ours, $\alpha = 0.3$)	72.51	73.76	74.60	73.85	85.69

4. CONCLUSION

In this paper, we employ CP as a principled uncertainty measure to guide data selection for human and model annotation in ATTA. To address the coverage gap of CP under domain shifts, we propose an adaptive weighting algorithm that enhances robustness and yields more reliable calibration across diverse environments. Our method improves efficiency of both human- and model-annotated data, reducing waste of scarce supervision while enabling more trustworthy pseudo-labels and stronger adaptation. Experiments show CPATTA achieves roughly 5% higher accuracy than SOTA ATTA methods. Future work includes developing better model update strategies and leveraging statistical distributions to characterize annotation errors in realistic deployment.

References

- [1] Tao Sun, Mattia Segu, Janis Postels, Yuxuan Wang, Luc Van Gool, Bernt Schiele, Federico Tombari, and Fisher Yu, “Shift: a synthetic driving dataset for continuous multi-task domain adaptation,” in *Proceedings of the IEEE/CVF conference on computer vision and pattern recognition*, 2022, pp. 21371–21382.
- [2] Guofa Li, Zefeng Ji, Xingda Qu, Rui Zhou, and Dongpu Cao, “Cross-domain object detection for autonomous driving: A stepwise domain adaptative yolo approach,” *IEEE Transactions on Intelligent Vehicles*, vol. 7, no. 3, pp. 603–615, 2022.
- [3] Ekaterina Kondrateva, Marina Pominova, Elena Popova, Maxim Sharayev, Alexander Bernstein, and Evgeny Burnaev, “Domain shift in computer vision models for mri data analysis: an overview,” in *International Conference on Machine Vision*. SPIE, 2021, vol. 11605, pp. 126–133.
- [4] Jonas Richiardi, Veronica Ravano, Natalia Molchanova, Pedro M Gordaliza, Tobias Kober, and Meritxell Bach Cuadra, “Domain shift, domain adaptation, and generalization: A focus on mri,” in *Trustworthy AI in Medical Imaging*, pp. 127–151. Elsevier, 2025.
- [5] Sining Sun, Binbin Zhang, Lei Xie, and Yanning Zhang, “An unsupervised deep domain adaptation approach for robust speech recognition,” *Neurocomputing*, vol. 257, pp. 79–87, 2017.
- [6] Shahram Ghorbani and John HL Hansen, “Domain expansion for end-to-end speech recognition: Applications for accent/dialect speech,” *IEEE/ACM Transactions on Audio, Speech, and Language Processing*, vol. 31, pp. 762–774, 2022.
- [7] Dequan Wang, Evan Shelhamer, Shaoteng Liu, Bruno Olshausen, and Trevor Darrell, “Tent: Fully test-time adaptation by entropy minimization,” in *International Conference on Learning Representations*, 2021.
- [8] Shuaicheng Niu, Jiaxiang Wu, Yifan Zhang, Yaofu Chen, Shijian Zheng, Peilin Zhao, and Mingkui Tan, “Efficient test-time model adaptation without forgetting,” in *International conference on machine learning*. PMLR, 2022, pp. 16888–16905.
- [9] Qin Wang, Olga Fink, Luc Van Gool, and Dengxin Dai, “Continual test-time domain adaptation,” in *Proceedings of the IEEE/CVF Conference on Computer Vision and Pattern Recognition*, 2022, pp. 7201–7211.
- [10] Shuaicheng Niu, Jiaxiang Wu, Yifan Zhang, Zhiqian Wen, Yaofu Chen, Peilin Zhao, and Mingkui Tan, “Towards stable test-time adaptation in dynamic wild world,” in *International Conference on Learning Representations*, 2023.
- [11] Shurui Gui, Xiner Li, and Shuiwang Ji, “Active test-time adaptation: Theoretical analyses and an algorithm,” in *International Conference on Learning Representations*, 2024.
- [12] Yaofu Chen, Shuaicheng Niu, Shoukai Xu, Hengjie Song, Yaowei Wang, and Mingkui Tan, “Towards robust and efficient cloud-edge elastic model adaptation via selective entropy distillation,” in *International Conference on Learning Representations*, 2024.
- [13] Guowei Wang and Changxing Ding, “Effortless active labeling for long-term test-time adaptation,” in *Proceedings of the Computer Vision and Pattern Recognition Conference*, 2025, pp. 25633–25642.
- [14] Anastasios N Angelopoulos and Stephen Bates, “A gentle introduction to conformal prediction and distribution-free uncertainty quantification,” *arXiv preprint arXiv:2107.07511*, 2021.
- [15] Glenn Shafer and Vladimir Vovk, “A tutorial on conformal prediction,” *Journal of Machine Learning Research*, vol. 9, no. 3, 2008.
- [16] Anastasios Nikolas Angelopoulos, Stephen Bates, Adam Fisch, Lihua Lei, and Tal Schuster, “Conformal risk control,” in *International Conference on Learning Representations*, 2024.
- [17] António Farinhas, Chrysoula Zerva, Dennis Thomas Ulmer, and Andre Martins, “Non-exchangeable conformal risk control,” in *International Conference on Learning Representations*, 2024.
- [18] Rina Foygel Barber, Emmanuel J Candes, Aaditya Ramdas, and Ryan J Tibshirani, “Conformal prediction beyond exchangeability,” *The Annals of Statistics*, vol. 51, no. 2, pp. 816–845, 2023.
- [19] Fatih Furkan Yilmaz and Reinhard Heckel, “Test-time recalibration of conformal predictors under distribution shift based on unlabeled examples,” *arXiv preprint arXiv:2210.04166*, 2022.
- [20] David Stutz, Krishnamurthy Dj Dvijotham, Ali Taylan Cemgil, and Arnaud Doucet, “Learning optimal conformal classifiers,” in *International Conference on Learning Representations*, 2022.
- [21] Goirik Chakrabarty, Manogna Sreenivas, and Soma Biswas, “A simple signal for domain shift,” in *Proceedings of the IEEE/CVF International Conference on Computer Vision*, 2023, pp. 3577–3584.
- [22] Da Li, Yongxin Yang, Yi-Zhe Song, and Timothy M Hospedales, “Deeper, broader and artier domain generalization,” in *Proceedings of the IEEE international conference on computer vision*, 2017, pp. 5542–5550.
- [23] Chen Fang, Ye Xu, and Daniel N Rockmore, “Unbiased metric learning: On the utilization of multiple datasets and web images for softening bias,” in *Proceedings of the IEEE international conference on computer vision*, 2013, pp. 1657–1664.
- [24] Dan Hendrycks and Thomas Dietterich, “Benchmarking neural network robustness to common corruptions and perturbations,” in *International Conference on Learning Representations*, 2019.
- [25] Kaiming He, Xiangyu Zhang, Shaoqing Ren, and Jian Sun, “Deep residual learning for image recognition,” in *Proceedings of the IEEE conference on computer vision and pattern recognition*, 2016, pp. 770–778.